ISSN 0105-8517

On the Stability of ADI Methods

Ole Østerby

DAIMI PB - 598
April 2016

DEPARTMENT OF COMPUTER SCIENCE
AARHUS UNIVERSITY
IT-parken, Aabogade 34
DK-8200 Aarhus N, Denmark

On the stability of ADI methods

Ole Østerby
Department of Computer Science
Aarhus University, Denmark.
oleby@cs.au.dk

Abstract

When solving parabolic equations in two space dimensions implicit methods are preferred to the explicit method because of their better stability properties. Straightforward implementation of implicit methods require time-consuming solution of large systems of linear equations, and ADI methods are preferred instead. We expect the ADI methods to inherit the stability properties of the implicit methods they are derived from, and we demonstrate that this is partly true. The Douglas-Rachford and Peaceman-Rachford methods are absolutely stable in the sense that their growth factors are ≤ 1 in absolute value. Near jump discontinuities, however, there are differences w.r.t. how the ADI methods react to the situation: do they produce oscillations and how effectively do they damp them. We demonstrate the behaviour on two simple examples.

Keywords: ADI, stability, growth factors, oscillations.
MSC 65M06, 65M12

1 Introduction

In this paper we study various finite difference methods for solving parabolic equations in two space dimensions:

$$u_t = P_1 u + P_2 u \tag{1}$$

where P_1 and P_2 are differential operators involving partial derivatives of orders 0, 1, and 2 in x and y, respectively. As a simple example we shall use $P_1 u = b_1 u_{xx}$ and $P_2 u = b_2 u_{yy}$ such that the equation is

$$u_t = b_1 u_{xx} + b_2 u_{yy} \tag{2}$$

The explicit method (**EX**) for solving (1) is

$$\Delta_t v^n = P_{1h}^n v^n + P_{2h}^n v^n$$

where P_{1h} and P_{2h} are finite difference operators approximating P_1 and P_2, respectively, and v is the finite difference approximation to the true solution u. In the case of (2) we have

$$\frac{v_{lm}^{n+1} - v_{lm}^n}{k} = b_1 \frac{v_{l+1,m}^n - 2v_{l,m}^n + v_{l-1,m}^n}{h_1^2} + b_2 \frac{v_{l,m+1}^n - 2v_{l,m}^n + v_{l,m-1}^n}{h_2^2}$$

where h_1, h_2, and k are the step sizes in the x-, y-, and t-direction, respectively, and l, m, and n are the corresponding step numbers. Here and in the following we shall use the notation of [8] (see pp. 6ff and pp. 103ff).
To study the stability we use the von Neumann approach ([1], [8], p. 23) and compute the growth factor

$$g_{EX}(\varphi) \;=\; 1 - 4b_1\mu_1 \sin^2\frac{\varphi_1}{2} - 4b_2\mu_2 \sin^2\frac{\varphi_2}{2}$$

where $\mu_1 = k/h_1^2$ and $\mu_2 = k/h_2^2$, and $-\pi \le \varphi_1, \varphi_2 \le \pi$. For stability we must have $|g(\varphi)| \le 1$ for all φ which puts severe restrictions on the time step size, in our case e.g.

$$b_i\mu_i \le \frac{1}{4} \quad \text{or} \quad k \le \frac{h_i^2}{4b_i}, \qquad i = 1, 2.$$

We notice in passing that the critical cases occur for φ_i close to $\pm\pi$. We call these solution components for *high-frequency* components because they correspond to solutions which oscillate between plus and minus at consecutive grid points (cf. [8], p. 21 and p. 57). Such components are dominant near a jump discontinuity, but are also introduced (with small amplitude) in continuous problems because of rounding errors. In these cases the condition $|g(\varphi)| \le 1$ is (necessary and) sufficient to keep such components small. Near a jump discontinuity we would prefer the growth factor to be smaller in absolute value in order to damp out the annoying oscillations.
In the following we shall use the short-hand notation

$$x_i \;=\; b_i\mu_i \sin^2\frac{\varphi_i}{2}, \qquad i = 1, 2,$$

and note that $0 \le x_i \le b_i\mu_i$, the maximum value to be attained for high frequency components.
To avoid the step size restrictions we might prefer the implicit method (**IM**) [5]:

$$\Delta_t v^n \;=\; P_{1h}^{n+1} v^{n+1} + P_{2h}^{n+1} v^{n+1}$$

whose growth factor

$$g_{IM}(\varphi) \;=\; \frac{1}{1 + 4x_1 + 4x_2} \tag{3}$$

satisfies $0 \le g(\varphi) \le 1$ implying absolute stability. To advance the solution one time step we must now solve a system of linear equations which is rather time-consuming. Instead we would prefer to use the Traditional Douglas-Rachford (**TDR**) ADI-method [3]:

$$\begin{aligned}(I - kP_{1h}^{n+1})\tilde{v} &= (I + kP_{2h}^{n})v^n \\ (I - kP_{2h}^{n+1})v^{n+1} &= \tilde{v} - kP_{2h}^{n} v^n\end{aligned}$$

which involves solving two tridiagonal systems of equations per time step. In the derivation of **TDR** ([8], p. 112) it appears that it is unnecessarily complicated. Another possibility which we shall call the Simple Douglas-Rachford (**SDR**) method has the same error order in time (= 1) and is written

$$\begin{aligned}(I - kP_{1h}^{n+1})\tilde{v} &= v^n \\ (I - kP_{2h}^{n+1})v^{n+1} &= \tilde{v}.\end{aligned}$$

The growth factor for **TDR** is ([8], p. 113)

$$g_{TDR}(\varphi) = \frac{1 + 16x_1x_2}{1 + 4x_1 + 4x_2 + 16x_1x_2} \tag{4}$$

and for **SDR**

$$g_{SDR}(\varphi) = \frac{1}{1 + 4x_1 + 4x_2 + 16x_1x_2} \tag{5}$$

The above-mentioned methods are only first order accurate in time. A second order method is the two-dimensional Crank-Nicolson (**CN**) method [2]:

$$\Delta_t v^n = \frac{1}{2}(P_{1h}^{n+1}v^{n+1} + P_{2h}^{n+1}v^{n+1}) + \frac{1}{2}(P_{1h}^n v^n + P_{2h}^n v^n)$$

The growth factor is

$$g_{CN}(\varphi) = \frac{1 - 2x_1 - 2x_2}{1 + 2x_1 + 2x_2} \tag{6}$$

and satisfies $-1 \leq g(\varphi) \leq 1$ again implying absolute stability.
To save computer time we again might prefer an ADI method, in this case Peaceman-Rachford (**PR**) [6]

$$\begin{aligned}(I - \frac{1}{2}kP_{1h}^{n+1})\tilde{v} &= (I + \frac{1}{2}kP_{2h}^n)v^n, \\ (I - \frac{1}{2}kP_{2h}^{n+1})v^{n+1} &= (I + \frac{1}{2}kP_{1h}^n)\tilde{v}\end{aligned}$$

with growth factor ([8], p. 110)

$$g_{PR}(\varphi) = \frac{(1 - 2x_1)(1 - 2x_2)}{(1 + 2x_1)(1 + 2x_2)}. \tag{7}$$

2 Stability and damping

In continuous problems high frequency components are introduced by rounding errors. They therefore have small amplitudes, and the requirement $|g(\varphi)| \leq 1$ is

perfectly satisfactory for keeping the amplitudes small. This is the case for all the above mentioned methods (with the exception of **EX**).
In problems involving a jump discontinuity the high frequency components have large amplitudes (cf. [8], p. 21). These components are effectively damped in the true solution (cf. [8], p. 23), and we would wish the same to be true for the numerical solution. Therefore we should like $g(\varphi)$ to be small for φ close to π.
Looking at the growth factor for **IM** (3) we note that $g_{IM}(\varphi)$ is small when x_1 and or x_2 is large, signalling that high frequency components are effectively damped. The same is true for **SDR**, but not for **TDR** where $g_{TDR}(\varphi)$ approaches 1 when both x_1 and x_2 are large.
The growth factor for **CN** approaches -1 when x_1 and/or x_2 is large. This means that high frequency components (which oscillate in x or y) will also oscillate in t, the well-known **CN**-oscillations. These oscillations are annoying but nevertheless give fair warning that the time step size is too large [4] and that certain measures should be taken to restore the physical significance of the numerical solution [7].
Looking at the growth factor for **PR** (7) we note that when x_1 *or* x_2 is large we have a similar situation with $g_{PR}(\varphi)$ approaching -1, but when both x_1 *and* x_2 are large then $g_{PR}(\varphi) \approx 1$ such that (as with **TDR**) high frequency components are slowly damped but with no 'wiggles' in time to reveal that fact.

3 Two test examples

To investigate in practice the properties of the above methods we study two examples based on equation (2) with $b_1 = b_2 = 1$ on the unit square with a jump discontinuity in the initial condition:

Example 1:
$$u(0,x,y) = \begin{cases} 1 & x < y \\ 0 & x = y \\ -1 & x > y \end{cases}$$

The boundary conditions for $t > 0$ are derived from the true solution:

$$u(t,x,y) = \frac{4}{\pi}\sum_{j=0}^{\infty}\frac{1}{2j+1}e^{-\frac{1}{2}\pi^2(2j+1)^2 t}\sin((2j+1)\frac{\pi}{2}(x-y+2)).$$

Example 2:
$$u(0,x,y) = \begin{cases} 1 & x < 0.5 \\ 0 & x = 0.5 \\ -1 & x > 0.5 \end{cases}$$

with the true solution

$$u(t,x,y) = \frac{4}{\pi}\sum_{j=0}^{\infty}\frac{1}{2j+1}e^{-4\pi^2(2j+1)^2 t}\sin((2j+1)2\pi x).$$

The step sizes in the x-, y-, and t-direction are $h_1 = h_2 = k = 0.025$ such that $\mu_1 = \mu_2 = 40$. In example 1 we have high-frequency solution components in both the x- and the y-direction at $t = 0$ and we therefore expect values of both x_1 and x_2 close to 40. In example 2 we only have a jump discontinuity when travelling in the x-direction and therefore only expect x_1 to be close to 40, while x_2 is small since any high frequency components in the y-direction will have very small amplitudes.

4 Results

Rather than presenting the complete two-dimensional solutions at each time step we have selected (typical) examples and show the solutions at specific lines close to the location of the jump. The results are shown in the following 6 figures. Each figure contains 6 curves, labeled **true**, **IM**, **TDR**, **SDR**, **CN**, and **PR**. Fig. 1–3 correspond to example 1 and Fig. 4–6 to example 2.
Fig. 1 and 4 show the x-dependence of $u(t, x, y)$ at the first time step, $t = 0.025$, for $y = 0.5$ and $0 \leq x \leq 1$,
Fig. 2 and 5 show $u(t, x, y)$ at the second time step, $t = 0.05$, for the same values of y and x, and
Fig. 3 and 6 show the t-dependence of $u(t, x, y)$ one x-step away from the jump at $x = 0.525$, $y = 0.5$, and $0 \leq t \leq 1$.
The findings confirm the predictions which can be made from the expressions for the growth factors.
In Example 1 where $x_1 \approx x_2 \approx 40$ both **IM** and **SDR** perform well (with **SDR** slightly better) whereas **TDR** shows a high frequency component (Fig. 1 and 2) which is very weakly damped ($g \approx \frac{25601}{25921} \approx 0.988$) (cf. Fig. 3). **CN** also shows a high frequency component which is damped with a negative g ($\approx -\frac{159}{161} \approx -0.988$) giving rise to the well-known wiggles in time (cf. Fig. 3) whereas **PR** has a positive g ($\approx (\frac{-79}{81})^2 \approx 0.951$) and has monotone behaviour in t. **SDR** is the winner with **IM** a close runner-up.
In Example 2 where $x_1 \approx 40$ and x_2 is small **IM**, **TDR**, and **SDR** perform equally well showing good damping of the high frequency components ($g \approx \frac{1}{161} \approx 0.006$). **CN** and **PR** both exhibit weakly damped oscillations due to negative growth factors. For **CN** $g \approx \frac{-79}{81} \approx -0.975$ and for **PR** slightly better, since the smallest value for φ_2 is not 0 but $\frac{\pi}{40}$ (cf. [8], p. 56) such that $x_2 \approx 40 \sin^2 \frac{\pi}{80} \approx 0.06$ and $g_{PR} \approx \frac{79}{81} \cdot \frac{0.88}{1.12} \approx 0.75$. After 10 steps the amplitude of the wiggles is reduced to 77% with **CN** and to 6% with **PR** (cf. Fig. 6).

References

[1] G. G. O'Brien, M. A. Hyman, and S. Kaplan, *A Study of the Numerical Solution of Partial Differential Equations*, J. Math. Phys., 29 (1951), pp. 223–251. doi:10.1002/sapm1950291223

[2] J. Crank and P. Nicolson, *A practical method for numerical evaluation of solutions of partial differential equations of the heat-conduction type*, Proc. Cambridge Philos. Soc., 43 (1947), pp. 50–67. Reprinted in Adv. Comput. Math., 6 (1996), pp. 207–226. doi:10.1007/BF02127704

[3] J. Douglas and H. H. Rachford, *On the numerical solution of heat conduction problems in two and three space variables*, Trans. Amer. Math. Soc., 82 (1956), pp. 421–439. doi:10.1090/S0002-9947-1956-0084194-4

[4] P. M. Gresho and R. L. Lee, *Don't suppress the wiggles – they're telling you something*, Computers and Fluids, 9 (1981), pp. 223–253. doi:10.1016/0045-7930(81)90026-8

[5] P. Laasonen, *Über eine Methode zur Lösung der Wärmeleitungsgleichung*, Acta Math., 81 (1949), pp. 309–317.

[6] D. W. Peaceman and H. H. Rachford, *The numerical solution of parabolic and elliptic differential equations*, J. SIAM, 3 (1955), pp. 28–41. doi:10.1137/0103003

[7] O. Østerby, *Five ways of reducing the Crank-Nicolson oscillations*, BIT, 43 (2003), pp. 811–822. doi:10.1023/B:BITN.0000009942.00540.94

[8] O. Østerby, *Numerical Solution of Parabolic Equations*, Department of Computer Science, Aarhus University, 2015 doi:10.7146/aul.5.5.

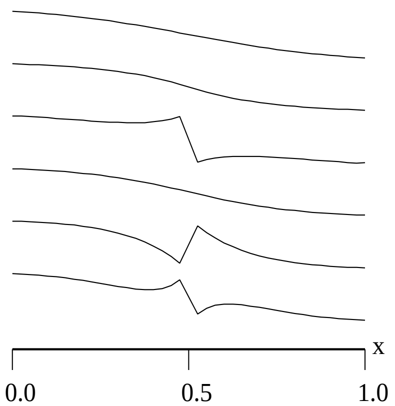

Fig. 1

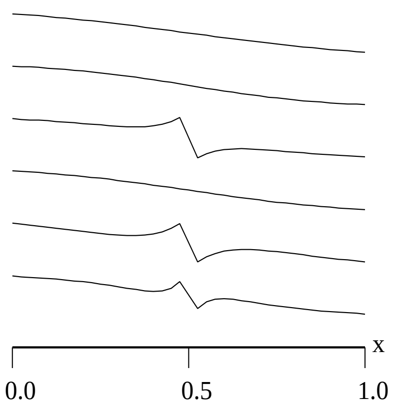

Fig. 2

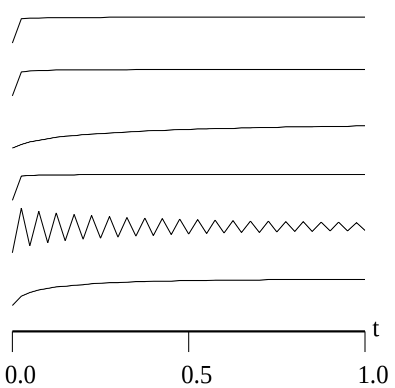

Fig. 3

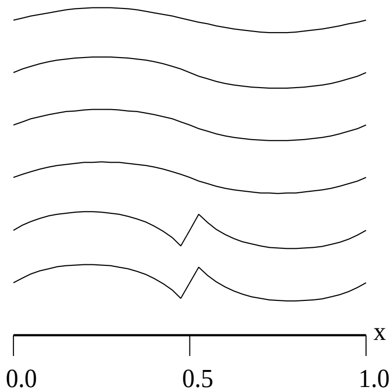

Fig. 4

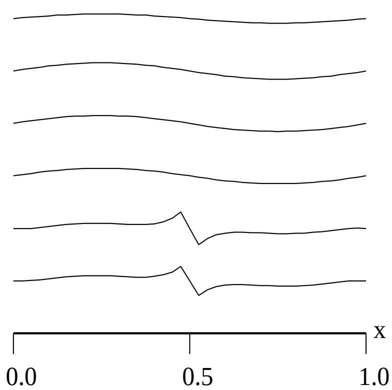

Fig. 5

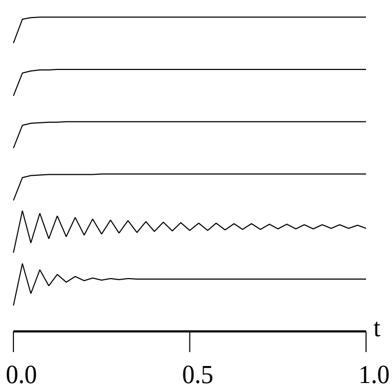

Fig. 6